Complicated Poincaré Half-Maps in a Linear System

Bernhard Uehleke and Otto E. Rössler

Institute for Physical and Theoretical Chemistry, University of Tübingen

Z. Naturforsch. **38 a,** 1107–1113 (1983); received June 18, 1983

Poincaré half-maps can be used to characterize the behavior of recurrent dynamical systems. Their usefulness is demonstrated for a linear three-dimensional single-loop feedback system. In this example everything can be calculated analytically. The resulting half-maps are "benign" endomorphic maps with a complicated topological structure. This is surprising since the combination of two such half-maps (yielding an ordinary Poincaré map) always implies simple behavior in a linear system. The method has a direct bearing on the theory of piecewise linear systems – like the well-known Danziger-Elmergreen system of hormonal regulation.

1. Introduction

The behavior of three-dimensional systems with oscillatory (or more generally, recurrent; see Birkhoff [1]) behavior is usually analyzed by considering a Poincaré map. This is a 2-dimensional cross section ("surface de section") through the trajectorial convolute (Poincaré [2]). In the classical Poincaré map, the observer considers only points produced by trajectories which successively puncture the Poincaré surface in one and the same direction.

Poincaré half-maps, in contrast, are defined not between an intersection point of the trajectory with the surface and the next passage through the same surface, in the same direction, but between the first intersection point and the very next passage through the same surface. This next passage crosses the surface in the opposite direction. Poincaré half-maps always contain nontransversal (tangential) curves. While bounded Poincaré maps can always be chosen in such a way as to be transversal everywhere (that is, to lack "tangential" punctur-ings; cf. Abraham and Robbin [3]), such tangenticity neccessarily occurs along some curve in any half-map.

Recently, a piecewise linear 3-dimensional system with smooth (C^1) trajectories was proposed as a prototypic system for the analytic study of chaotic behavior in the three dimensions (Rössler [4]). Such an analysis can be performed using Poincaré half-maps (Uehleke [5]).

In the following, results pertinent to an ordinary linear system wil be represented. They can easily be applied to piecewise linear systems. Specifically, we will be interested in the two Poincaré half-maps that belong to the two halves of a linear system whose state space is divided by an arbitrary separating plane.

2. The System

We consider the simplest linear single-loop feedback system in three dimensions:

$$\dot{x} = -x + \alpha z - \alpha, \quad \dot{y} = x - y, \quad \dot{z} = y - z, \quad (1)$$

where α is a real parameter. Different values of α produce different kinds of qualitative behavior of the system. In the special case of $\alpha = -8$, for example, we have the linear phase-shift oscillator of both electronics (cf. [6]) and reaction kinetics (Seelig and Göbber [7]). The geometric picture of the trajectories in phase space looks as follows: There exists a "center" in a 2-dimensional planar invariant manifold which is spanned by the complex conjugate eigenvectors. The central point of this planar set of concentric ellipses is the steady state s of the system. This point is also traversed by the second invariant manifold (the one-dimensional one corresponding to the real-negative eigenvalue).

If α is assumed somewhat smaller or larger than -8, the center is turned into a (stable or unstable, respectively) "focus". The trajectories inside the planar eigenmanifold are no longer closed, but rather spiral inwards or outwards, respectively.

Reprint requests to Prof. O. E. Rössler, Institute for Physical and Theoretical Chemistry, University of Tübingen, Auf der Morgenstelle 8, 7400 Tübingen, West Germany.

0340-4811 / 83 / 1000-1107 $ 01.3 0/0. – Please order a reprint rather than making your own copy.

For arbitrary values of α, further topological types of behavior are possible. Arnold [8] showed that there exist 11 different topological types in 3-dimensional systems. In the present case, one obtains only 6 topological types since only a single parameter (α) is allowed to be varied (cf. [5]).

In the following, just one of these 6 types will be considered: the one corresponding to values of $\alpha < -8$. In this case the flow inside the planar eigenmanifold is unstable (positive real part of the pair of complex-conjugate eigenvalues) while the motion inside the one-dimensional invariant eigenmanifold is stable (negative real eigenvalue).

Every trajectory of the system moves within an invariant 2-dimensional manifold. Using reduced coordinates, all invariant manifolds become rotation symmetric to the real (one-dimensional) eigenvector a. The reduced coordinates a, b, c are defined by

$$\begin{pmatrix} a \\ b \\ c \end{pmatrix} = \begin{pmatrix} 1/(3H^2) & 1/(3H) & 1/3 \\ -1/(3H^2) & -1/(3H) & 2/3 \\ -1/(2QH^2) & 1/(2QH) & 0 \end{pmatrix} \cdot \begin{pmatrix} x - x_s \\ y - y_s \\ z - z_s \end{pmatrix}.$$

where $x_s = y_s = z_s = \alpha/(\alpha - 1)$. Using these transformations, (1) becomes

$$\begin{aligned} \dot{a} &= (1 - H)\, a, \\ \dot{b} &= (1 - H/2)\, b - QHc, \\ \dot{c} &= QHb - (1 + H/2)\, c, \end{aligned} \tag{2}$$

where $Q = \sin(\pi/3)$ and $H = (\alpha)^{(1/3)}$.

Since (2) is an uncoupled system, the solutions can be written down easily. Eliminating time and introducing the cylindrical variable $r = \sqrt{b^2 + c^2}$, one obtains all of the two-dimensional invariant manifolds (which are now rotation symmetric):

$$r(a) = r_0 \left(\frac{a}{a_0}\right)^{\left(\frac{-1-H/2}{-1+H}\right)} + r_0\, a_0^{\left(\frac{1+H/2}{-1+H}\right)} a^{\left(\frac{-1-H/2}{-1+H}\right)}. \tag{3}$$

with $r_0 > 0$ and $a_0 \neq 0$ chosen arbitrary. Geometrically, these manifolds look like a family of concentric "trees" that posses divergent "foots" (since the radius r becomes infinite as the "tree" approaches the planar eigenmanifold $a = 0$, the "tree basis").

The whole family of invariant trees described by (3) is now to be "cut" in an oblique manner by a horizontal plane. In the original coordinates, the plane of interest to be chosen may be $z = 1$, for example. This plane becomes

$$a + b + 1/(H^3 - 1) = 0 \tag{4}$$

in the reduced coordinates. Note that the assumed restriction to a constant z-value does not restrict topological generality.

Inserting (3) into (4) gives the intersection lines of the invariant manifolds (trees) with the cutting plane. These intersection lines have the equation

$$c(a) = \pm\sqrt{r^2(a) - b^2(a)} = \pm\sqrt{r^2(a) - (1 - z_s - a)^2}. \tag{5}$$

They can easily be transformed back into original coordinates ($x, y; z = 1$). This then yields the following picture (Fig. 1).

One clearly sees the "yearly rings" of a beautiful tree that is cut in an oblique manner. In accordance with this interpretation, there is a family of ellipse-shaped closed curves ("isolae") around a core point. This family of closed curves is bounded by a singular "Cartesian leaf"-shaped curve (with double point C). Outside, there is a second family of curves that are no longer closed but have the form of the Greek capital letter Omega [4].

In the same plane $z = 1$, there exists a single "nontransversal line". It is the straight line defined by $y = 1$. Its nontransversality is easy to check: By inserting $y = 1$, $z = 1$ into (1), one obtains $\dot{z} = 0$, which means that the spiralling trajectories of the system are moving tangentially to the plane $z = 1$ along this line. This line is the only set of points in the plane where this occurs.

Beyond that line (that is, in the region $y > 1$), all trajectories are moving upwards ($\dot{z} > 0$) through the

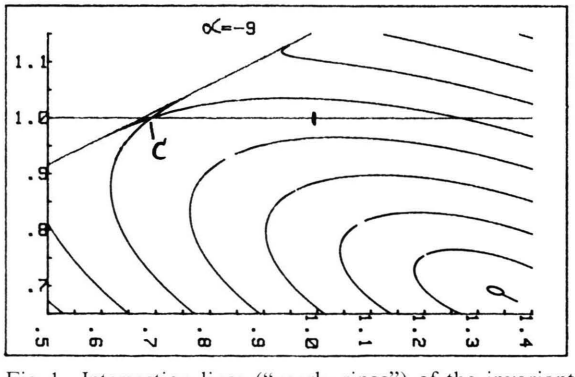

Fig. 1. Intersection lines ("yearly rings") of the invariant manifolds ("trees") of the system of (1) with the plane $z = 1$. Abscissa: x. Ordinate: y.

plane $z = 1$, while in front of that line ($y < 1$), all trajectories are moving downwards ($\dot{z} < 0$). It now appears to be natural to adopt the following terminology: the half system with $z < 1$ is to be called the "underwater" half system and the other (with $z > 1$), the "air" half system, with the separating plane $z = 1$ being the "water surface".

3. Special Points of the Underwater Half-Map

Every "diving" trajectory, originating from some value $y < 1$ in the water surface $z = 1$, is mapped by the underwater half system onto the other half region $y > 1$ of the water surface. Specifically, points lying on a yearly ring (Fig. 1) are mapped onto other points lying on the same ring, but in the other half of the water surface. By considering all yearly rings, we will be able to construct the whole half map.

Let us first consider points of the (nonclosed) Omega curves. Here a simple diffeomorphic mapping from the part of the curve with $y < 1$ onto the other part (with $y > 1$) applies. This case is shown in Figure 2a. The nontransversal point lying on the horizontal line $y = 1$ is a fixed point.

Proceeding to the case of the (closed) isolae, it is perhaps best to consider first those not touching or crossing the line $y = 1$ (see Figure 2b). The image of these isolae lies on the nearly straight line in the foot of the tree (see Figure 1).

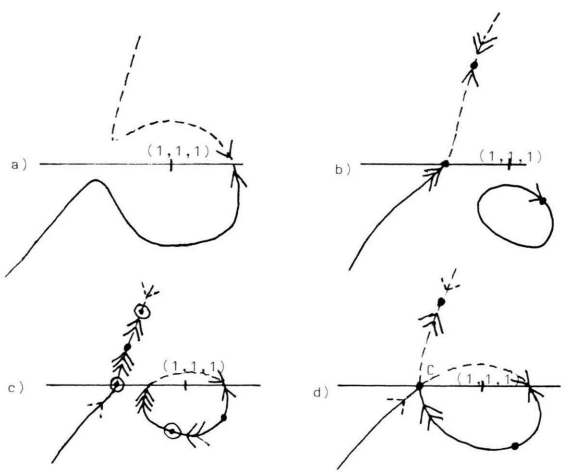

Fig. 2. a)–d) Mapping of some yearly rings by the underwater half-system (from the diving down part ——, onto the emerging part – – –, of the water surface). For the special points, see text. (In *c*, add one more dark dot on the horizontal line at the tip of the triple arrow.)

Since the latter line is not closed, there necessarily exists a special point on each isola with the property that one of its neighborhoods is mapped to one end of the foot line (namely, to the "beginning" of its upper portion on the line $y = 1$), while the other neighborhood is mapped onto a more distant part of the same line. This special point of the isola (with non-unique image) renders the underlying mapping an (almost everywhere bijective) endomorphic map rather than a diffeomorphic one. As shown in Fig. 2b, the frontal portion of the nearly straight foot line (with $y < 1$) is mapped diffeomorphically onto the other side of the inserted segment.

Larger isolae, large enough to cross the line $y = 1$, behave in a more complicated fashion. As shown in Fig. 2c, here only one part of the isola has its image inserted in the foot line. The other part has its image on the other part of the isola itself (with $y > 1$).

The Cartesian curve can be considered as a limit case of a large isola. It possesses essentially the same behavior (see Figure 2d).

What are the common properties of the "special points" on all these curves? First of all, there is the point (1, 1, 1) which is the tangential point of that (single) isola which touches the line $y = 1$ (compare Figure 1). Inserting this point into (1) yields $\dot{y} = 0$. Points of the line $y = 1$ lying to the left ($x < 1$) and to the right ($x > 1$) of this point, respectively, have differing topological properties under the half map. All trajectories that become tangential to the plane $z = 1$ have to do so somewhere on the line $y = 1$. But those becoming tangential in the range $x > 1$ are touching down from the air in order to start through anew (with some neighbors becoming submerged very briefly) while those becoming tangential in the left-hand range ($x < 1$) are welling up from the depth and are diving down again thereafter. This happens because the line $y = 1$ is tangential to every tree. In the left-hand range ($x < 1$) of the line, the trees are being touched in their dorsal (upper) parts – which means that the tangential trajectories come from below. The right hand range corresponds to tangencies in the ventral part of the trees. At the point (1, 1, 1), a vertical tangential plane applies to the corresponding tree – with the consequence that the tangential trajectory is exactly horizontal.

In the "uncritical" (right-hand) range, trajectories diving down in a neighborhood of the line $y = 1$

(with $y < 1$) will emerge to the other side of the same line, but still close to it. In the critical (left-hand) range, in contrast, neighboring trajectories will after diving down emerge in a distant region – making at least one full underwater turn in the meantime.

The image of the critical part of the line $y = 1$ forms a "critical curve", as it may be called. This curve may consist of several segments, in dependence on the value of α and (as a consequence) on the number of underwater turns involved in the generation of the different segments.

Every pair of "jump points" in between two segments of the critical curve (black dots in Fig. 2c) is generated by one special trajectory. These special trajectories are horizontally touching the water surface $z = 1$ exactly twice. The twice touching trajectories are making either one or more turns around the tree axis in between their two touchings of the water surface.

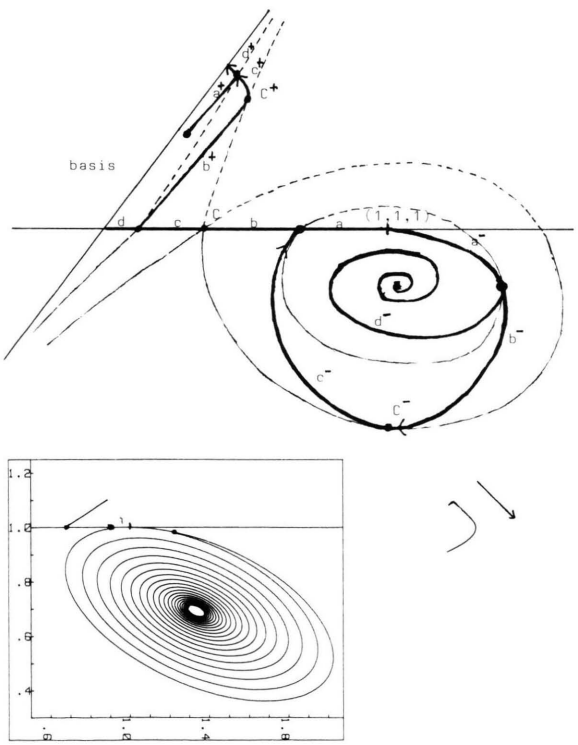

Fig. 3. a) and b) Image (+) and pre-image (−) of the critical (bold) part of the line $y = 1$. a, b, c, d = different segments of that part (cf. text). a) Qualitative picture. (Two yearly rings are also shown in thin lines.) ● = points of the single "twice tangential" trajectory. ■ (at the tips of the arrows) = pre-image of the tree basis, corresponding to the intersection point of the water surface with the tree axis. b) Quantitative picture. See text. The inset gives a blown-up view (arrow) of the hook-shaped criticed curve to the left.

Analogously, the *pre*-images (images under *negative* time) of the (left-hand) critical part of the line $y = 1$ also result in a critical curve, which is located in the region of the isolae. This critical curve consists of the same number of segments again. Taken together, these segments form the "critical spiral".

The pre-images of the uncritical part of the line $y = 1$, in contrast, are again points of that line itself. We already saw that these points are fixed points.

The picture of Fig. 3 summarizes the details. The straight bold line refers to the critical portion of the line $y = 1$. Both the images (+) and the pre-images (−) of its different parts (labeled a to d) are also shown in bold. The case shown applies to $\alpha = -9$. It would have been possible to give a simpler picture (with the critical curve consisting of a single segment only) if another parameter had been chosen (for example, $\alpha = -10$).

However, an even more complicated picture applies when more than one doubly tangential trajectory exists (in which case each additional trajectory of this type makes one more underwater turn). In the limit α approaches from below the value $\alpha = -8$, the number of doubly tangential trajectories becomes infinite.

It is easy to see that a triply tangential trajectory cannot exist, because the upper side of each slanted tree is tangential to the plane $z = 1$ (at the line $y = 1$) in at most two points. (There is one tree where these two points fall into one, namely the Cartesian point.)

If the number of doubly tangential trajectories is m, the number of segments of the critical curve is $m + 1$. This is because the end points of the segments are generated by the special (doubly tangential) trajectories. The critical curves can be indicated analytically in the form of an implicit equation (see [5]).

4. Topology of the Underwater Half Map

The critical curves are "separating" in the sense that whole two-dimensional regions, traversed by them, are mapped onto disconnected regions by the underwater half-system. Conversely, all regions not traversed by a critical curve are mapped onto a connected region in a diffeomorphic fashion (except for the boundary points). The resulting overall map is

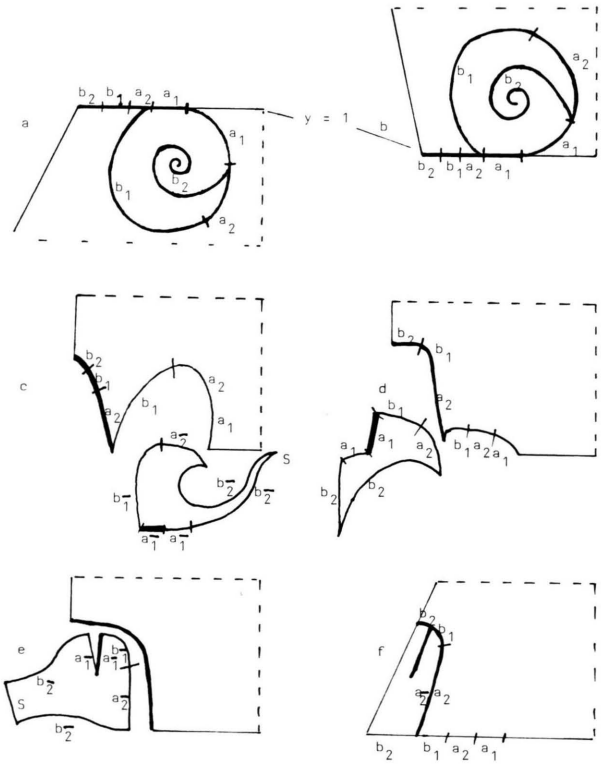

Fig. 4. a)–f) Stepwise derivation of the half-map of the underwater system. a) Original ("diving down") domain. b)–f) Different stages in the transformation (distortion).

shown in Figure 4. It was obtained by first cutting the plane along all the critical curves (Fig. 4a), then flipping it over along the line $y = 1$ (Fig. 4b), and then topologically distorting it in an almost everywhere diffeomorphic manner.

The only nondifferentiable part of the distortion occurs in the step from d to e in Fig. 4: The point S in d (the lowerleft most cusp) is blown up becoming the line S in e. The image f is related to the original a in a fashion that is qualitatively similar to the well known baker's transformation invented by Hopf [9]. There too, an originally connected region is bijectively transformed (except for a line segment) into a number of disconnected, individually diffeomorphic pieces. (In the baker's transformation there are only two pieces present each generated by a linear mapping.)

5. The Upper-Water System ("Air System")

Let us now look at the other half-map in the present linear system. One obtains a mapping from the part lying behind the line $y = 1$ of the water surface onto the frontal part (with $y < 1$). This time, it is the right-hand portion ($x > 1$) of the line $y = 1$ which is the critical part. The mapping of the critical part by the "air" half-system again yields a critical curve (the arc a^+) in Figure 5.

From the topology of the yearly rings (only two of them have been entered in the Figure), one sees that the whole half plane $y > 1$ (to the right of the tree basis) is mapped onto the "triangle" that is

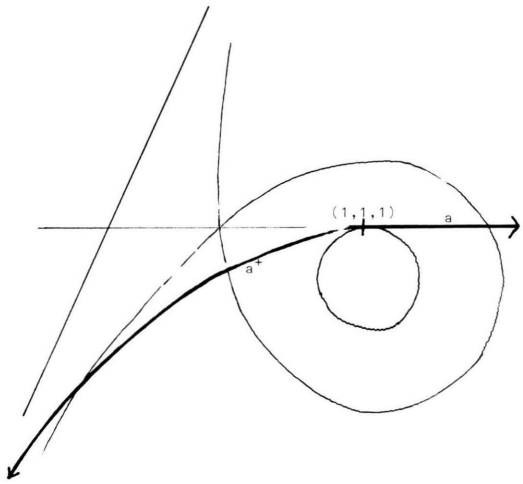

Fig. 5. Image of the critical (bold) part of the line $y = 1$ of the "air" half-system. Note that there is no pre-image present in the plane $z = 1$. For the analogous picture of the underwater half-system, see Figure 3a.

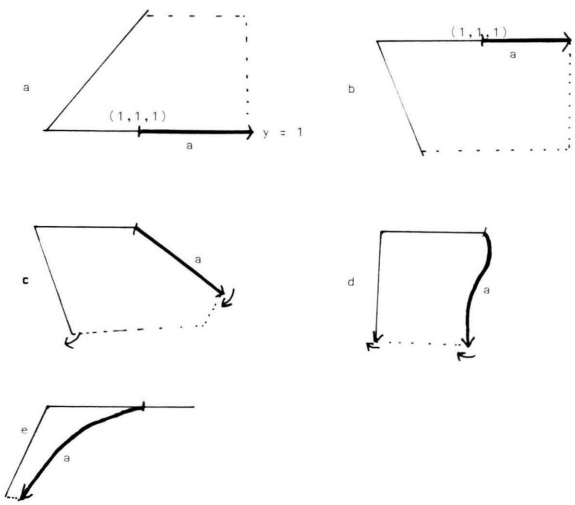

Fig. 6. a)–e) Stepwise derivation of the half-map of the air system. Cf. also Figure 4.

formed by the tree basis, the line $y = 1$, and the arc, respectively (Figure 5). Except for the boundaries, this mapping is a diffeomorphism for $\alpha < -8$. Figure 6 shows the underlying distortion process in analogy to Figure 4.

The present map is obviously much simpler than that generated by the underwater system. The remaining problem, to be discussed next, is how to combine both maps.

6. Combining Both Half Maps

Combining the above two half-maps (Figs. 4 and 6) is not very easy because of the complexity of the underwater half-map. On the other hand, a simple, fully diffeomorphic Poincaré maß was at first expected to apply to any oscillating linear system. As it turns out, this is not the case.

Each of the two half-maps can be characterized by an implicit function F the solution of which gives the next penetration point on the Poincaré surface [5]. In a fully linear system, the implicit function is the same for both half systems (that is, $F_{\text{underwater}} = F_{\text{air}}$). This allows one to combine the two steps by computing one solution of the implicit function F only: One simply looks at the second iterate of the given implicit function, that is, for the second zero of F.

A geometric picture of the resulting combined map is shown in Figure 7. To our surprise, it still possesses the complex shape familiar from the underwater part. We conclude that simple linear systems show complex Poincaré maps on Poincaré surfaces that do not cut right through the steady state.

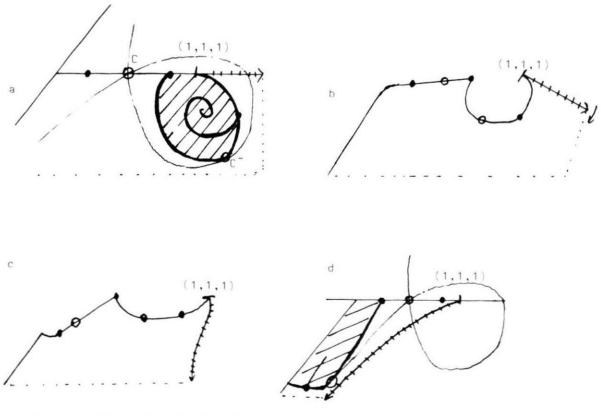

Fig. 7. Topological shape of the whole Poincaré map. Stepwise derivation as in Figs. 4 and 6. Symbols as in Figs. 3 and 4. Note that the cross-hatched portion is completely analogous to Figure 4.

7. Discussion

It has been shown that a Poincaré map of a fully linear system may possess a rather complicated topological structure that is closely related to the structure of one of its half-maps. This finding may be taken as an indication that Poincaré half-maps may be useful also in more complicated systems. Half-maps have already been of use in the investigation of piecewise linear systems [5].

The class of picewise linear systems promises new insights into the nature of chaos. All other analytically tractable chaos-producing systems of differential equations are much more "singular" than this class. The other two cases are singular-perturbation-type chaos (Rössler [10]; Takens [11]) and ordinary perturbation-type chaos (Mel'nikov [12]).

Piecewise linear systems may become popular again. The prototypic example is the chaotic modification of the Danziger-Elmergreen [13] system [14], [4]; see also [15, 16]. Here $\alpha = -8.4$ in the underwater half-system and $\alpha = 160$ in the air system, for example. A thorough analysis of the topologically different ways how chaos can be generated in this system on the basis of the half-maps of Fig. 4 was attempted in [5].

An interesting open problem is the following: What happens to a linear system (possessing – as we saw – complicated Poincaré maps) when it is changed by a C^1 perturbation into a piecewise linear system that is still arbitrarily close to the linear system. This class of piecewise linear systems should still possess a topologically complicated cross section, even if the latter does not show up either in simulations or in the omega limit set of the system. The most urgent problem is wether "chaotic separatrices" exist. Higher-dimensional piecewise linear, arbitrarily close to linear, systems may possibly even possess chaotic attractors.

Acknowledgements

O. E. R. thanks Ralph Abraham for a discussion on chaotic separatrices and Bill Smith for stimulation.

[1] G. D. Birkhoff, Nouvelles Recherches sur les Systèmes Dynamiques. Memoriae Pont. Acad. Sci. Novi. Lyncae, S. 3, **1,** 85 (1935).
[2] H. Poincaré, Acta Math. **13,** 1 (1880).
[3] R. Abraham and J. Robbin, Transversal Mappings and Flows, Benjamin, New York 1967.
[4] O. E. Rössler, The Gluing-together Principle and Chaos, in: Nonlinear Problems of Analysis in Geometry and Mechanics (M. Attaia, D. Bancel, and I. Gumowski, eds.), Pitman, Boston-London 1981, pp. 50–56.
[5] B. Uehleke, Chaos in einem stückweise linearen System: Analytische Resultate. Ph.D. thesis, University of Tübingen 1982.
[6] O. E. Rössler, A Synthetic Approach to Exotic Kinetics, in: Physics and Mathematics of the Nervous System (M. Conrad, W. Güttinger, and M. Dal Cin, eds.), Springer Lecture Notes in Biomath. **4,** 546 (1974).
[7] F. F. Seelig, and F. Göbber, J. Theor. Biol. **30,** 485 (1971).
[8] V. I. Arnold, Differential equations, Springer-Verlag, Berlin 1980.
[9] E. Hopf, Ergodentheorie, Springer-Verlag, Berlin 1937, p. 42.
[10] O. E. Rössler, Z. Naturforsch. **31 a,** 259 (1976).
[11] F. Takens, Implicit Differential Equations: Some Open Problems, Springer Lect. Notes in Math. **535,** 237 (1976).
[12] V. K. Mel'nikov, Trans. Moscow Math. Soc. **12,** 1 (1963).
[13] L. Danziger and G. L. Elmergreen, Bull. Math. Biophys. **18,** 1 (1956).
[14] R. Rössler, F. Götz, and O. E. Rössler, Biophys. J. **25,** 216a (1979).
[15] C. Sparrow, J. Math. Anal. Appl. **83,** 275 (1981).
[16] P. Glendinning and C. Sparrow, Local and global behavior near homoclinic orbits, Preprint 1983.